



A new method for continuous measurements of oceanic and atmospheric N₂O, CO and CO₂: performance of off-axis integrated cavity output spectroscopy (OA-ICOS) coupled to non-dispersive infrared detection (NDIR)

D. L. Arévalo-Martínez¹, M. Beyer¹, M. Krumbholz¹, I. Piller^{1,*}, A. Kock¹, T. Steinhoff¹, A. Körtzinger¹, and H. W. Bange¹

¹Helmholtz Centre for Ocean Research Kiel (GEOMAR), Düsternbrooker Weg 20 24105 Kiel, Germany

* now at: Institute of Physical Chemistry at the Christian-Albrechts-Universität Kiel, Max-Eyth-Str. 2 24118 Kiel, Germany

Correspondence to: D. L. Arévalo-Martínez (darevalo@geomar.de)

Received: 20 June 2013 – Published in Ocean Sci. Discuss.: 26 July 2013

Revised: 6 November 2013 – Accepted: 7 November 2013 – Published: 11 December 2013

Abstract. A new system for continuous, highly resolved oceanic and atmospheric measurements of N₂O, CO and CO₂ is described. The system is based upon off-axis integrated cavity output spectroscopy (OA-ICOS) and a non-dispersive infrared analyzer (NDIR), both coupled to a Weiss-type equilibrator. Performance of the combined setup was evaluated by testing its precision, accuracy, long-term stability, linearity and response time. Furthermore, the setup was tested during two oceanographic campaigns in the equatorial Atlantic Ocean in order to explore its potential for autonomous deployment onboard voluntary observing ships (VOS). Improved equilibrator response times for N₂O (2.5 min) and CO (45 min) were achieved in comparison to response times from similar chamber designs used by previous studies. High stability of the OA-ICOS analyzer was demonstrated by low optimal integration times of 2 and 4 min for N₂O and CO respectively, as well as detection limits of <40 ppt and precision better than 0.3 ppb Hz^{-1/2}. Results from a direct comparison of the method presented here and well-established discrete methods for oceanic N₂O and CO₂ measurements showed very good consistency. The favorable agreement between underway atmospheric N₂O, CO and CO₂ measurements and monthly means at Ascension Island (7.96° S 14.4° W) further suggests a reliable operation of the underway setup in the field. The potential of the system as an improved platform for measurements of trace gases was explored by using continuous N₂O and CO₂ data to characterize the development of the seasonal equatorial

upwelling in the Atlantic Ocean during two R/V *Maria S. Merian* cruises. A similar record of high-resolution CO measurements was simultaneously obtained, offering, for the first time, the possibility of a comprehensive view of the distribution and emissions of these climate-relevant gases in the area studied. The relatively simple underway N₂O/CO/CO₂ setup is suitable for long-term deployment onboard research and commercial vessels although potential sources of drift, such as cavity temperature, and further technical improvements towards automation, still need to be addressed.

1 Introduction

The assessment of marine emissions of climate-relevant gases has become a critical issue in the attempt to improve our current understanding of the impacts of the ocean on atmospheric composition and chemistry and therefore, on climate. Atmospheric concentrations of long-lived greenhouse gases such as nitrous oxide (N₂O) and carbon dioxide (CO₂) have been increasing at unprecedented rates over the last century, mainly in association with human activities, leading to an overall warming of the Earth's climate system (Denman et al., 2007). Both N₂O and CO₂ are strong greenhouse gases (Forster et al., 2007), while carbon monoxide (CO) is considered to be an indirect greenhouse gas that alters the tropospheric photochemistry and enhances the concentrations

of other important reactive gases such as methane and ozone (Bates et al., 1993; Prather et al., 2001). Despite their importance, vast areas of the ocean remain uninvestigated by observational studies of these gases, and for other areas, temporal and spatial resolution of the observations is coarse due to constraints posed by the sampling intervals that can be achieved by using discrete and semi-continuous methods, leading to large uncertainties in marine emissions estimates especially in the cases of N₂O and CO (Nevison et al., 1995; Stubbins et al., 2006).

In this context, the development and implementation of cost-effective methods for underway measurements (providing data at frequencies in the order of minutes or even seconds) offers the potential to extend the spatial coverage and temporal resolution of ship-based observations. The recent development of sensitive analytical techniques based on infrared detection such as cavity ringdown spectroscopy (CRDS), enhanced integrated cavity output spectroscopy (ICOS) and off-axis integrated cavity output spectroscopy (OA-ICOS) has enabled the detection of a number of trace gases in nanomolar concentrations and opened the possibility of obtaining continuous measurements for a variety of applications, including soil and atmospheric monitoring (Baer et al., 2002; Kasyutich et al., 2003; Maddaloni et al., 2006) as well as for surveys of the surface ocean onboard research vessels (Becker et al., 2012; Greife and Kaiser, 2013) and ships of opportunity (Gülzow et al., 2011, 2013). This represents a great improvement compared to conventional detection techniques (mainly based upon gas chromatography) due to the strongly increased temporal resolution that can be achieved. Theoretical basis and technical considerations of CRDS and ICOS as well as a comparison with the OA-ICOS approach are presented elsewhere (Mazurenka et al., 2005; Friedrichs, 2008).

Within this set of available techniques, OA-ICOS is particularly interesting due to its high mechanical robustness and relatively simple optical configuration, which make it suitable for long-term measurements in the field. In OA-ICOS the laser alignment with respect to the optical cavity is such that the spatial separation between multiple modes (transmitted frequencies) is increased (Baer et al., 2002; Dyroff, 2011). The spacing between modes in the cavity defines the free spectral range (FSR) which, if kept lower than the laser bandwidth, produces enhanced sensitivity. With the above-described setup, reflections impacting on each side of the cavity appear as dots forming elliptical patterns that after several rebounds result in a very dense mode spectrum (Herriot et al., 1964; Paul et al., 2001) and consequently a low FSR, thus explaining the improved sensitivity of OA-ICOS based analyzers. Despite the fact that similar sensitivity can be achieved with CRDS and ICOS, the associated technical requirements pose difficulties when it comes to obtaining data in a high temporal resolution. These constraints seem to be addressed using OA-ICOS because of a comparatively simple configuration and insensitivity to vibration and mis-

alignments (Maddaloni et al., 2006), which highlights the potential advantage of implementing OA-ICOS to perform high-quality at-sea measurements of climate-relevant trace gases.

Here, we present for the first time a system capable of performing combined, continuous, and high-resolution oceanic and atmospheric measurements of N₂O, CO and CO₂. This was achieved by coupling an OA-ICOS analyzer and a non-dispersive infrared analyzer (NDIR) to a shower-head (Weiss-type) equilibrator. The combined setup underwent several laboratory tests in order to assess aspects such as precision, accuracy, long-term stability, linearity and response time. Furthermore, it was employed during two oceanographic campaigns in the equatorial Atlantic Ocean to test its performance and to explore its potential for autonomous deployment onboard voluntary observing ships (VOS).

2 Instrumentation and methods

2.1 Instrumentation

N₂O and CO measurements were carried out by a DLT-100 N₂O/CO analyzer (Los Gatos Research, Inc., USA) which provides simultaneous measurements of molar fractions of these gases as well as water vapor (H₂O) with precision at sub-ppb level. The device is based upon the OA-ICOS technology which combines the use of a high-finesse optical cavity with a continuous-wave, narrow-band laser aligned in an off-axis configuration (Fig. 1). A detailed description of the instrument can be found in Baer et al. (2002) and therefore its essential functioning is only briefly described here: an infrared diode laser beam ($\Delta\nu < 1$ MHz) is continuously injected into a stainless-steel, cylindrical, 0.28 m long cavity (volume 400 cm³) which is sealed by a pair of highly reflective (99.99 %) mirrors. Since the laser is not oriented at a right angle with respect to the cavity, the number of absorption paths produced is significantly increased, resulting in an enhancement of the detected signal (O'Keefe and Deacon, 1988; Maddaloni et al., 2006). The final product is a temporally integrated transmitted light intensity which is then transferred to a digital oscilloscope interfacing with a standard internal computer. User interface for data visualization, calibration and other configuration settings consist of a screen on top of the bench and an incorporated keyboard/mouse pad.

During operation, sample air is continuously pumped through the detection cell (cavity) using an internal pump at low flow rates (Lo mode) or an external pump at high flow rates (Hi mode). In the Lo mode the gas sample is directed through an electronic pressure controller placed before the inlet of the cavity, thereby providing isolation from ambient variations in pressure and possible changes in pumping speed. In this study, the system was set up in the Lo mode with a measured gas flow rate of 235 mL min⁻¹ and a

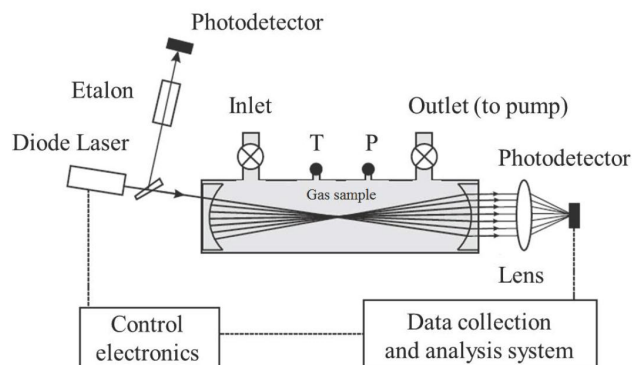


Fig. 1. Schematic diagram of an instrument based upon OA-ICOS (after Baer et al., 2002). The gas sample is conducted continuously through the cavity while the laser beam bounces multiple times between the highly reflective ($\sim 99.99\%$) mirrors. “T” and “P” represent the cell’s temperature and pressure sensors, respectively.

gas pressure of about 106 mbar. Furthermore, all the internal gas connectors were replaced by stainless steel Swagelok[®] fittings because the original parts were not gas-tight. The cell’s temperature and pressure are continually recorded by the instrument and are used as part of the gas molar fraction calculations.

A calibration routine is carried out by flushing the cavity with a standard gas mixture of known N₂O and CO concentrations, and the system automatically self-calibrates to the input values. As mentioned before, the DLT-100 measures the H₂O molar fraction along with N₂O and CO. This allows the calculation of the dry mole fractions of N₂O and CO, thus accounting for the bias in partial pressure due to the water vapor content of the gas sample (Burch et al., 1962). In order to calculate the dry mole fractions of N₂O and CO, the DLT-100 software performs the following calculation:

$$x(\text{gas})_{\text{dry}} = \frac{x(\text{gas})_{\text{wet}}}{\left(1 - \frac{x_{\text{H}_2\text{O}}}{10^6}\right)}, \quad (1)$$

where $x(\text{gas})_{\text{dry}}$ and $x(\text{gas})_{\text{wet}}$ are the molar fractions of the corresponding gas after and before the correction, respectively, and $x_{\text{H}_2\text{O}}$ is the measured molar fraction of water vapor. Further procedures in order to correct for band broadening effects are possible and have been proven to be stable at different CO concentrations (Zellweger et al., 2012). However, prior drying of the gas sample avoids the need of such corrections and therefore it has been adopted as a customary practice during the measurements (see Sect. 2.3).

For CO₂ measurements a NDIR gas analyzer LI-6252 (LI-COR Biosciences, Inc., USA) was used. The instrument functions based on the detection of differential infrared radiation (IR) absorption in two cells; one cell contains the sample of interest (sample cell) whereas the other contains a gas of known CO₂ content (reference cell). The reported

concentration is proportional to the IR absorption difference between them. Temperature and pressure within the cell need to be monitored in order to accurately calculate mole fractions of CO₂. The LI-6252 bears a sensor to measure temperature directly in the cell, whereas for pressure measurements, an external high-precision ($<0.05\%$) pressure transducer (SETRACERAM[®], model 270) was installed at the outlet of the analyzer such that the analog signal was transmitted to it. The calculations performed by the analyzer’s software to determine the CO₂ concentrations as well as the internal calibration functions are detailed in the instruction manual (LI-COR, 1996). Small output drifts need to be corrected on a daily basis by adjusting zero and span potentiometers while flushing the cell with CO₂-free synthetic air and the highest standard gas concentration available, respectively. Since the LI-6252 does not include an H₂O detection channel, air is dried before being flushed into the cells in order to avoid errors associated with dilution and band broadening effects (McDermitt et al., 1993; Hupp, 2011). Readings were obtained by means of a Matlab[®] script running on a standard laptop interfaced to the instrument via serial port. The averaging interval is set to 10 s in order to obtain a low noise level.

2.2 Equilibration system

In order to determine the dissolved content of trace gases in seawater, most systems require the analyte to be in gas phase rather than in liquid phase (Johnson, 1999). For this purpose, various designs of equilibrators have been developed and used in conjunction with continuous (Körtzinger et al., 2000) and semi-continuous (Bange et al., 1996b; Stubbins et al., 2006) systems for gas measurements; these are particularly suitable since a virtually infinite volume of sample seawater can be directed through the chamber and subsequently analyzed.

A smaller version of the Weiss-type equilibrator (Butler et al., 1988) is used to obtain an equilibrated gas phase to be measured by the N₂O/CO and CO₂ analyzers. It consists of an acrylic chamber (height: 25 cm, diameter: 15 cm) which is filled with seawater until a headspace of about 3 L is reached. A circular plate with holes is placed on the upper side just beneath the water inlet, such that the water dribbles down through the headspace. The lower part contains the water phase which effectively isolates the headspace into the chamber and is continuously renewed with the ship’s water supply system. During operation, the sample air is constantly drawn from the headspace, flows through the analyzers and then returns back to the chamber, forming a closed loop. In order to avoid differences with respect to the ambient pressure, the headspace is vented to the atmosphere by means of a Teflon[®] tube connected to the upper part of the chamber. The estimated error for N₂O and CO₂ measurements using this type of equilibrator is about 0.2 % or less, whereas for CO the error can be as high as 25 % (Johnson, 1999). This

difference for CO can be explained by its low solubility and the large gradient between oceanic and atmospheric mixing ratios, since it enhances the effect of potential venting of ambient air into the chamber (Conrad et al., 1982; Bates et al., 1995).

2.3 Combined setup

A schematic drawing of the underway system is shown Fig. 2. Both analyzers are installed in sequence, forming a closed circuit in which equilibrated air circulates through the detectors and flows back to the equilibration chamber with a flow rate of 235 mL min⁻¹. Previous tests indicated that no pressure variations are caused on the LI-6252 cell by the action of the internal pump of the DLT-100, and therefore no errors due to pressure differences are expected from the setup itself. Furthermore, both instruments are synchronized to Coordinated Universal Time (UTC) in order to assure temporal comparability of the results, although the measuring interval remains different, being 1 s for the DLT-100 and 10 s for the LI-6252. During operation, the water stream is continuously pumped through the equilibrator at a rate of about 2 L min⁻¹. Sample air is dried stepwise by conducting it first through a glass cold trap inserted into a 2 L Dewar flask (KWG Isotherm) partially filled with ice, and then through a Nafion[®] tube (model MD-070-72F-4). The H₂O molar fraction in the dried air is about 6000 ppb and it is accounted for during the final computations (cf. Eq. (1)). After drying, the sample air flows towards the control unit and ultimately towards the analyzers before it returns to the equilibrator. A Pall Acro[®] 50 air filter with pore size 0.2 μm is installed between the drying elements and the control unit in order to prevent water residuals from reaching the instruments. Teflon[®] (PTFE) tubing is used to draw all the connections between the equilibrator and the control unit and to the analyzers. The equilibration temperature is measured by placing an EASYLOG 40KH temperature logger (±0.01°C) inside the equilibrator, while the equilibration pressure is assumed to be very close to atmospheric pressure since the headspace is permanently vented to ambient air. Pressure readings are taken from the ship's data distribution system.

The control unit contains all the stainless steel valves (Swagelok[®]) used to regulate the air flow through the gas lines switching between equilibrator, ambient and standard gases. These valves are operated manually and have different configurations of opening/closing depending on the gas being measured. It is worth noting, however, that no matter which combination is used, there must always be air flowing towards the analyzers because the DLT-100 is sensitive to strong pressure differences that may arise from the total closure of the gas line. A 3-way valve is used to separate the equilibrator gas circuit from the atmospheric air/standard gases circuit (Fig. 2).

Ambient air is pumped at a rate of 350 mL min⁻¹ using an Air Cadet[™] pump (Thermo Scientific), dried using the same

approach as for the gas stream from the equilibrator and then conducted through the gas analyzers. In this case, a control valve is switched to prevent air from the equilibrator from passing through the Nafion[®] tube. In field applications the great distance between the air intake and the location of the system might create difficulties for a proper flushing of the lines. Therefore, during ambient-air measurement, the pump is always switched on approximately 5 min before the measurements are taken in order to ensure a complete flushing of the intake gas lines. In contrast to the headspace air, ambient air is discarded via a three-way valve which is configured to direct the flow to a 2 m long plastic hose which is open to the laboratory air.

In order to account for possible drifts of the system (DLT-100) and to calibrate final data (LI-6252), control measurements of standard gas mixtures of N₂O, CO and CO₂ in synthetic air as well as compressed air are performed at regular intervals. The standard gases used (Std.1: 362.3 ± 0.2 ppb N₂O, 233.5 ± 0.3 ppb CO, 200.0 ± 0.1 ppm CO₂; Std.2: 746.0 ± 0.2 ppb N₂O, 255.5 ± 0.3 ppb CO, 602.0 ± 0.1 ppm CO₂) were prepared by Deuste Steininger GmbH (Mühlhausen, Germany) and calibrated at the Max Planck Institute for Biogeochemistry (Jena, Germany) against the National Oceanic and Atmospheric Administration (NOAA) standard scale. The exhaust gas from the control measurements is also discarded like the ambient air by switching the three-way valve to “waste” position.

During field deployment, ambient air and control measurements are conducted every 6 h over a period of approximately 5 min for each gas. Zero and span adjustments for the LI-6252 are conducted every 24 h by using synthetic air and the standard 2, whereas the DLT-100 calibration is made every two weeks. As a result, each 6 h period of seawater measurements is bracketed by control measurements of standard gases, thus allowing for further correction procedures of the raw data before final computations are made.

3 Assessment of system performance

3.1 Response time of the equilibrator

A given gas phase in equilibrium with the underlying water phase in the equilibrator chamber is assumed to adjust to changing water properties within a time frame given by the response time for the gas of interest. This re-equilibration process is mainly dependent on factors such as the type of chamber, water flow and the solubility of the different gases (Johnson, 1999). The time constant of the equilibrator, τ , defined here as the time interval needed for a given concentration difference between water and gas phases to decrease exponentially to 1/e of the initial value, was determined experimentally and is used as an indicator of the chamber's performance. For this, a step experiment was carried out by using two reservoirs of water with different N₂O concentrations.

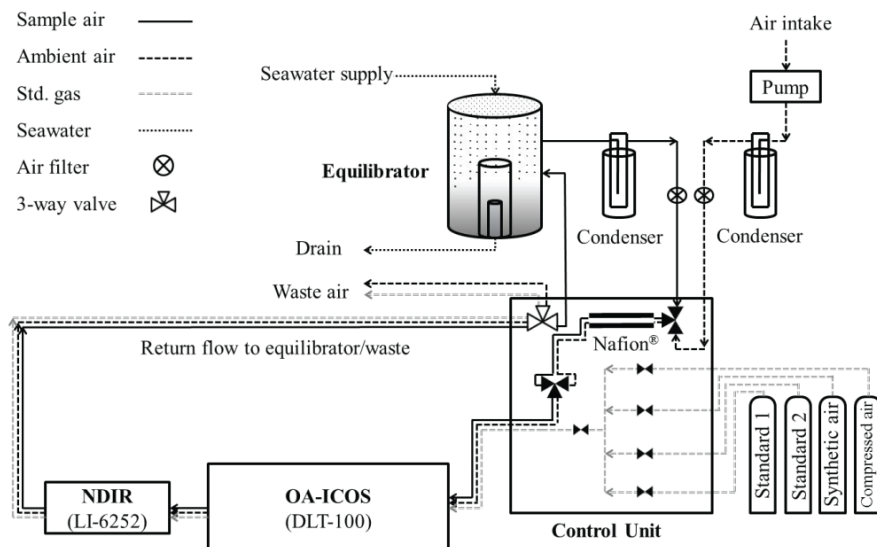


Fig. 2. Schematic drawing of the analytical system used for underway N₂O, CO and CO₂ measurements. Arrows indicate the direction of the gas/water flows.

In order to produce distinct N₂O levels, two 100 L tanks were filled with freshwater, and while one of them was exposed to ambient (laboratory) air (N₂O = 402.4 ppb), the other was manipulated by aeration with a standard gas for approximately 3 h until a N₂O molar fraction of 570 ppb was reached. The water from the tanks was supplied to the equilibrator by means of a three-way valve, thus allowing a rapid switching between reservoirs. Moreover, a control valve was installed before the equilibrator's inlet to sustain a water flow of about 2 L min⁻¹.

Water from both reservoirs was successively conducted through the equilibrator until steady readings were achieved (SD < 0.2 ppb). Once stable readings were obtained for the enhanced concentration reservoir, the flow was switched to the second reservoir with lower concentration and the change was continuously recorded. Assuming that the re-equilibration of the headspace gas follows first-order kinetics, the process can be described by the following equation (Körtzinger et al., 1996):

$$\frac{dp_g}{dt} = k(p_w - p_g), \quad (2)$$

where p_g and p_w are the N₂O concentrations in the gas and water phases, respectively, and k is equivalent to τ , an indicator of how fast the equilibrator responds to changes in the gas concentration of the water phase. Integration of Eq. (2) yields the following exponential equation:

$$p_g = p_w + (p_g^0 - p_w) e^{-\tau t}, \quad (3)$$

with p_g^0 and p_w being the N₂O concentrations of the enhanced and ambient air reservoirs, respectively, and p_g the

recorded gas concentration at a given time, t . The time constant τ can be calculated from the slope of the change in N₂O concentration over time after arranging Eq. (3). A plot of $-\ln(p_g - p_w / p_g^0 - p_w)$ vs. time shows a strong linear correlation, justifying the assumption that first-order kinetics govern the equilibration process (Fig. 3). The step experiment was repeated several times and resulted in a value of 145 ± 20 s (approx. 2.5 min) for τ . A much larger τ was found for CO during the same experiment, indicating that the equilibration process for this gas takes ca. 45 min. Such difference is expected due to the low solubility of CO in seawater (Wiesenburg and Guinasso, 1979) and it has been observed before for a similar equilibrator by Johnson (1999). The values predicted from that study are much larger (6.4 min N₂O and 216.3 min CO), which might be due to the different size of the equilibration chamber. Since the equilibrator in our system is comparatively small, the volume of headspace gas that needs to be equilibrated with the water stream is lower, thus enhancing the speed of the process.

Due to the similar solubilities of N₂O and CO₂ (Weiss, 1974; Wilhelm et al., 1977; Weiss and Price, 1980) we assume that the time constant for both gases is also comparable under the same setup. This result lies within the range of observations from step experiments carried out at different CO₂ concentrations in equilibrators of distinct designs, with time constants that vary between 0.76 min and 3.76 min (Körtzinger et al., 1996; Gülzow et al., 2011). Likewise, the obtained values for τ were in the same range as those reported by Butler et al. (1988) and Weiss et al. (1992) for a similar Weiss equilibrator. Thus it can be stated that the equilibrator performs well, responding fast enough to achieve

measurements of gases like N₂O and CO₂ on minute-scale temporal resolution. On the other hand, such fine resolution for CO measurements is constrained by CO's low solubility, which delays the equilibrium process. However, in this case the major oceanic sources (microbial and photochemical production) and sinks (microbial consumption and air-sea gas exchange) alter the concentrations of CO over periods of several hours (Kitidis et al., 2011), and therefore the features of diurnal variability can still be detected by the DLT-100 when coupled to the equilibrator. Further improvement of the temporal resolution for CO measurements with this method could be achieved by enhancing the equilibration process with equilibration chambers that bear a higher exchange surface and increased water flow.

3.2 Precision and accuracy

The quality of any system's high-sensitivity measurements is largely determined by the system's stability, because this dictates for how long the produced signal can be averaged before drift effects influence the data. Here, the concept of Allan variance (σ_A^2) is used to characterize the system's stability and short-term precision (Allan, 1966). For a given set of adjacent measurements, σ_A^2 tends to decrease with increasing integration times as long as random noise dominates over instrumental drift. When higher integration times are considered, however, drift tends to increase and σ_A^2 starts to rise, indicating a reduced performance of the system. This means that during the time phase dominated by random noise, σ_A^2 is equivalent to the statistical variance of the measurements and therefore its square root provides an estimation of the detection limit (Werle et al., 1993; Kroon et al., 2007). Since the LI-6252 and similar models are well-established instruments that have been extensively tested as part of autonomous systems for CO₂ measurements (Pierrot et al., 2009) the analysis here is centered on the DLT-100 analyzer.

Continuous measurements of a gas with molar fractions of 362.73 ± 0.59 ppb N₂O and 233.32 ± 0.46 ppb CO (mean \pm SD) over a period of 15 min and a sampling rate of 1 Hz were used to calculate σ_A^2 . Subsequently σ_A^2 was plotted against the integration time and as can be seen in Fig. 4 minimum σ_A^2 was attained at integration times of 120 s and 240 s for N₂O and CO, respectively. These values correspond to the optimal integration times for the analyzer. Even though at higher integration times drift tends to increase, the DLT-100 has been found to be stable within ± 0.6 ppb N₂O and ± 0.4 ppb CO over a time period of 5 h (not shown). Similar optimal integration times (2–5 min) were obtained for CO with an OA-ICOS based analyzer by Zellweger et al. (2012), with values being stable within ± 0.1 ppb over a 10 h period.

By making use of the Allan standard deviation (σ_A), i.e. the square root of the minimum σ_A^2 , the detection limit of the system can be estimated (Werle et al., 1993). Thus, for $\sigma_A^2 = 1.4 \times 10^{-3}$ ppb² N₂O and $\sigma_A^2 = 5.9 \times 10^{-4}$ ppb² CO the corresponding detection limits of the DLT-100 are 37 ppt

for N₂O and 24 ppt for CO. Detection limits in the order of 50 and 60 ppt have been reported for N₂O measurements using quantum cascade laser (QCL) spectrometers (Nelson et al., 2004; Kroon et al., 2007). On the other hand, our values are higher than the 10 ppt detection limit reported by Zellweger et al. (2012) for CO measurements with the same type of OA-ICOS analyzer. Nevertheless, the obtained results still satisfy the high standard requirements proposed for instruments used in sensitive measurements of trace gases (Nelson et al., 2004) and feature improved detection limits compared to QCL instruments.

Nelson et al. (2004) suggested a value of 1 ppt of the ambient mixing ratio as the optimal precision to be achieved for highly sensitive field measurements of N₂O. With an ambient mixing ratio of 320 ppb, this is equivalent to a precision of $0.3 \text{ ppb Hz}^{-1/2}$. An estimate of the short-term precision of the DLT-100 was obtained by means of the expression:

$$\sigma = \sigma_A \cdot f_s^{-1/2}, \quad (4)$$

where σ_A is the Allan standard deviation in ppb and f_s is the sampling frequency in Hz. Precisions of $3.8 \times 10^{-2} \text{ ppb Hz}^{-1/2}$ for N₂O and $2.4 \times 10^{-2} \text{ ppb Hz}^{-1/2}$ for CO were achieved. These values are comparable to those reported for other OA-ICOS analyzers using the same measurement rate (Hendriks et al., 2008; Zellweger et al., 2012), and are lower compared to those obtained by Kroon et al. (2007) for a QCL analyzer operated at 10 Hz ($0.5 \text{ ppb Hz}^{-1/2}$). The results also evidence an improvement in the precision achieved for N₂O and CO measurements by employing OA-ICOS in comparison with the use of gas chromatographic methods (Weiss, 1981; Bates et al., 1995; Bange et al., 1996a). Altogether the stability and high precision of the DLT-100 analyzer, capable of detecting concentration changes in the sub-ppb range, makes it suitable not only for continuous long-term monitoring of N₂O and CO, but also for detailed surveys of fine structure features of their distribution and fluxes.

3.3 Long-term stability of the calibration

Continuous deployment of the DLT-100 in the field supposes the need of low maintenance and also requires the instrument to deliver stable results for extended periods of time. In order to test the instrument's stability after calibration, standard gases with different molar fractions were measured at fixed intervals (5 min) for 14 days. At the beginning, the analyzer was calibrated by using a reference gas containing 362.3 ppb N₂O and 233.5 ppb CO, and subsequently the gases were supplied in increasing concentration order at five instances. A 3 min average was calculated for each gas (SD < 0.2 ppb) and the results were used to quantify the offset of the measurements with respect to the standard values by using

$$\text{MD} = \frac{M - S}{S}, \quad (5)$$

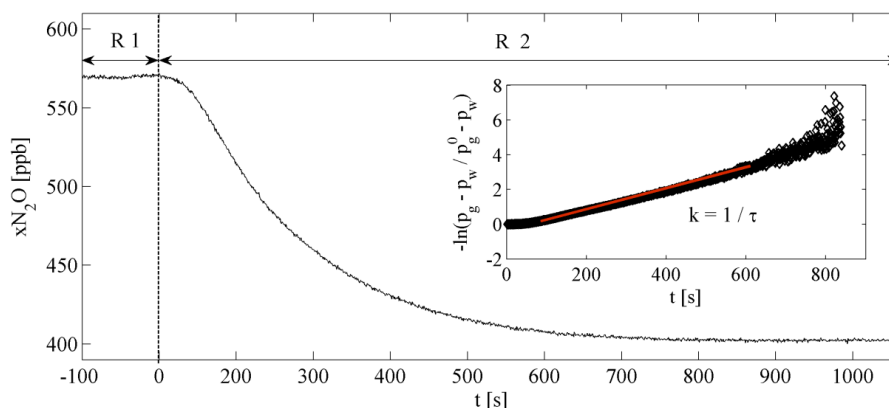


Fig. 3. Results of the step experiment carried out to determine the response time of the equilibrator. Water from the high-concentration reservoir (R 1) was conducted through the equilibrator until stable readings were obtained and at $t = 0$, the flow was switched to the ambient air reservoir (R 2). A plot of the linearized change in N₂O concentration over time was used to calculate the time constant, τ . The red line depicts the regression line of the data.

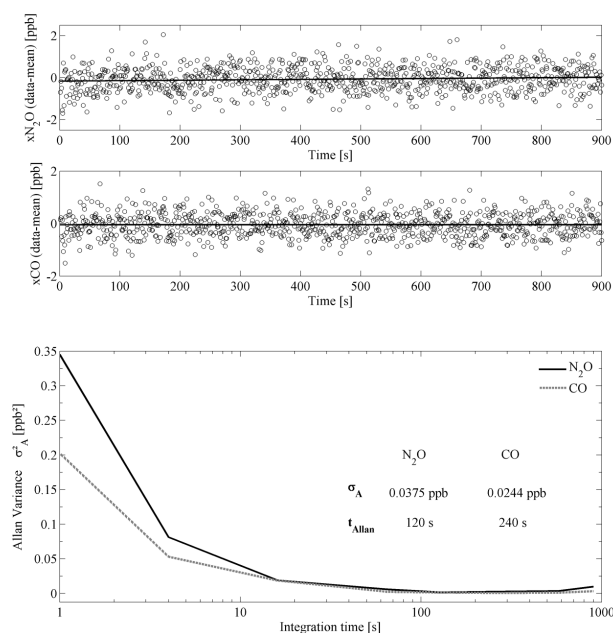


Fig. 4. Instrument drift test of the DLT-100 analyzer. Upper panel shows a time series of molar fractions of N₂O and CO over a 15 min period at a rate of 1 Hz. The results are presented as single data point deviations from the mean value, and the corresponding linear regression lines are also depicted. The Allan variance plot for N₂O and CO over the measurement period is shown in the lower panel, including the values of Allan standard deviation (σ_A) and optimal averaging times (t_{Allan}) at the minimum σ_A^2 .

where M and S are the measured and standard gas values in ppb, respectively. No significant drift for N₂O was observed during the 2 weeks, with highest deviations being lower than 0.2 % and a maximum of 1 % due to occasional concentration changes in the order of 2 ppb (Table 1). For CO the de-

viations were somewhat higher, mainly due to uncertainties on the concentration of the reference gases. Nevertheless, the observed drift for CO remained within less than 2 % during the first week and increased only on the last days due to mole fraction differences on the order of 3–4 ppb. Furthermore, a two-point calibration factor was computed for each measurement period by means of:

$$F_{cal} = \frac{S_H - S_L}{M_H - M_L}, \quad (6)$$

with S_H and S_L being the highest (746.0 ppb N₂O) and lowest (322.5 ppb N₂O) standard values, respectively, and M_H and M_L being the corresponding highest and lowest measured values (3 min average). This factor was calculated only for N₂O since the concentration difference between CO standards was only 20 ppb. A mean value of 1.01 for F_{cal} with variations smaller than 0.1 % during the measurement period evidenced the high accuracy of the DLT-100. Based on these results it can be stated that, upon calibration, the instrument provides N₂O and CO measurements without significant drift for a period of at least two weeks. Accuracy in N₂O measurements was slightly lower for the high concentration standard (746.0 ppb) during the experiment mainly due to the fact that the values are further apart from the single calibration point of the instrument. Such an effect does not impair the DLT-100 general performance and the measurements are highly accurate, although at even higher concentration ranges a more frequent calibration might be necessary.

3.4 Linearity

The linearity of the DLT-100 was assessed by preparing dilutions of standard gases in synthetic air and measuring them sequentially for 10–15 min periods. The desired dilutions were achieved by means of two mass flow controllers (redy smart series, Vögtlin Instruments AG, accuracy ± 0.3 %)

Table 1. Results of the calibration experiment carried out over a 14-day period. The MD values (cf. Eq. (5)) calculated from 3 min averages of measurements for each standard gas are presented.

Date and time	N ₂ O (ppb)			CO (ppb)	
	322.5	362.3	746.0	233.5	255.5
21/12/2010 10:52:02	0.094 %	-0.0055 %	-0.70 %	0.13 %	1.08 %
21/12/2010 15:34:07	0.050 %	0.017 %	-0.80 %	0.11 %	1.11 %
22/12/2010 12:58:07	-0.200 %	-0.130 %	-0.97 %	0.04 %	0.77 %
29/12/2010 13:50:36	0.047 %	0.075 %	-0.85 %	1.16 %	1.35 %
03/01/2011 10:11:32	0.057 %	0.140 %	-0.81 %	1.16 %	1.78 %

connected to the analyzer while interfacing with the commercially available software EasyHTK (HTK Hamburg GmbH, Germany) that produced gas mixtures with the targeted concentrations. Two sets of dilutions were done so as to cover the upper and lower boundaries of the operational range of the instrument (at which the instrument's response is expected to be linear). The first set of dilutions encompassed the range between 0 and 750 ppb N₂O, and a quadratic function was found to better fit the response of the DLT-100 within that concentration interval (top panel, Fig. 5). It is worth noting, however, that the regression residuals showed only slight departures from linearity, and therefore the quadratic term only improves the residuals by <0.001 % (linear fit: $y = 0.99x + 1.47$, $r^2 = 0.9998$). Thus, in practical terms, the analyzer's results might as well be regarded as linear for N₂O. Recently, Zellweger et al. (2012) performed a similar test on the same type of analyzer and also found a quadratic function to be more appropriate to characterize the instrument response during CO measurements (regression residuals within ± 0.2 ppb).

The second set of dilutions was prepared in the range between 2800 and 4000 ppb, in order to assess the response of the DLT-100 when exposed to high levels of N₂O and CO like those found in places of strong outgassing to the atmosphere (Bange et al., 1996b; Kitidis et al., 2011). Figure 5 (bottom panel) shows the results of this test, wherein the DLT-100 performance is also best characterized by a quadratic fit for both N₂O and CO. Like in the lower concentration range, the linear approach also represents the response of the analyzer for both gases well (linear fits: N₂O $y = 1.02x + 87.57$, $r^2 = 0.9999$; CO $y = 0.94x + 61.43$, $r^2 = 0.9999$). Thus it can be inferred from these observations that the response of the DLT-100 is rather uniform in both the lower and upper boundaries of its operational range for N₂O and CO, and that it can be best represented by quadratic functions.

4 At-sea tests

The underway system was deployed during two oceanographic campaigns to the equatorial Atlantic Ocean on board

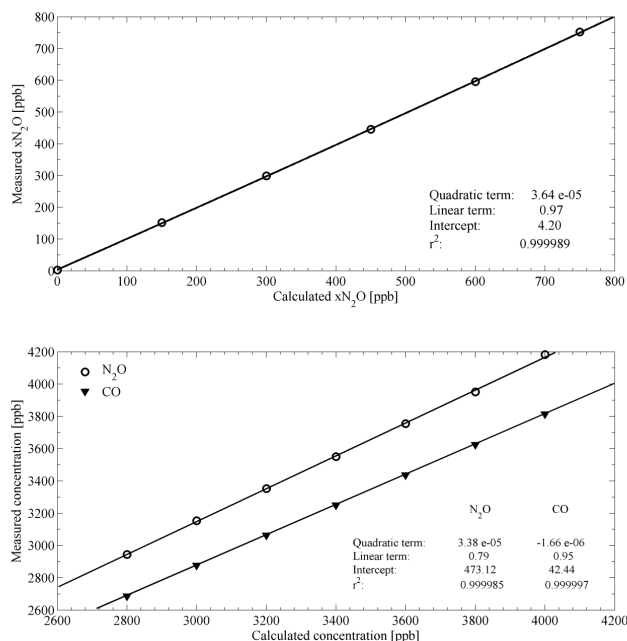


Fig. 5. Plots of the linearity tests performed on the DLT-100 analyzer. Regression lines of the corresponding quadratic fits applied are depicted. The upper panel shows a linearity plot for N₂O on the concentration range of 0 to 750 ppb and the lower panel the corresponding plot for N₂O and CO on the concentration range between 2800 and 4000 ppb.

of the R/V *Maria S. Merian* (MSM 18 legs 2 and 3, May–July 2011, Fig. 6). Seawater was taken from the ship's water supply system (centrifugal pump) which draws water from two inlets at the bottom of the vessel at approximate 6 m depth, and it was continuously pumped through the equilibrator at a rate of 2 L min⁻¹. Atmospheric measurements were accomplished by pumping ambient air from the ship's mast at approximately 30 m height and leading it to the system by means of polyethylene/aluminum tubing (Synflex® 1300) at a rate of 350 mL min⁻¹. A detailed description of the measurement setup is given in Sect. 2.3.

As depicted in Fig. 7, standard gas measurements made every 6 h over a period of 64 days evidenced only slight drifts

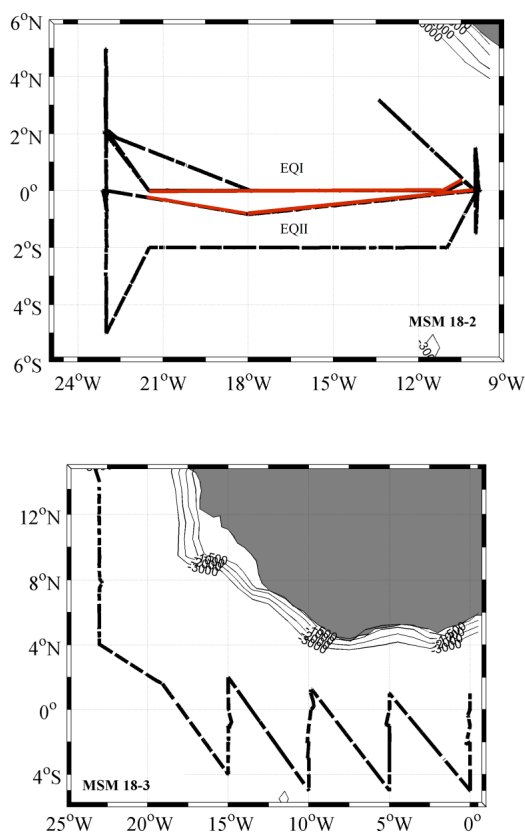


Fig. 6. Cruise tracks of the R/V *Merian* MSM 18-2 and 18-3 cruises. The red lines indicate two equatorial sections carried out before (EQI) and after (EQII) the onset of the equatorial upwelling (see Sect. 5 and Fig. 10).

of the DLT-100 for N₂O (mean offset = 0.005 ppb). Most measurements fluctuated within 1 % of the standard value (362.3 ppb N₂O) with a maximum of 1.4 %, and no discernible trend of increase or decrease was found over the time spanned by the two cruises. Similar results were obtained for CO during MSM 18-2 with stable values within ± 1 % of the reference gas (233.5 ppb CO). In the course of MSM 18-3, however, high scatter was observed with deviations as high as 5 % (10 ppb CO) indicating a strong decrease in accuracy. Given that the DLT-100 did not exhibit such problem during laboratory tests carried out after the cruises, it is unlikely that this bias was the result of malfunctioning of the laser or presence of particles on the cavity. Instead, marked changes in ambient temperature could have driven the steep changes in the detected signal of CO during MSM 18-3. From the time series of CO and temperature data recorded by the DLT-100 during both cruises, it can be seen that the strong temperature changes after 1 July do indeed coincide with elevated (though highly variable) CO values for the standard gas during MSM 18-3. Analysis of N₂O and temperature data for the same period indicated that the effect is considerably lower for

N₂O, with maximum drift values of ca. 3 ppb for the same temperature change (6 °C). In contrast to these results, Zellweger et al. (2012) found only slight deviations from standard gas measurements of CO (−0.4/+1.1 ppb) while using the same type of analyzer during temperature manipulations under controlled conditions. Although the simulated temperature changes during their tests were on the same order of magnitude of the observed changes during MSM 18-3, they spanned a much lower range of temperatures than our field observations (32–38 °C), and therefore may not be directly comparable. Overall, these results suggest that although the analyzer is stable over long time periods, care must be taken to ensure that there is proper ventilation and that corrections are developed to account for the effects of temperatures close to the upper boundary of the analyzer's recommended operating temperature (35 °C). Enhanced performance models of this analyzer include an internal thermal control system but those were not tested as part of this study.

The performance of the N₂O/CO/CO₂ system in the field was evaluated by comparison with well-established methods. Since no discrete method for CO measurements was available during the cruises, the assessment was done based on N₂O and CO₂ data and only underway CO data are presented. Discrete samples were taken on a daily basis from a bypass connected to the same water source that supplied the underway system. For N₂O, a modification of the analytical method by Bange et al. (2001) was applied. Triplicate samples were collected in 20 mL brown glass flasks which were rinsed twice before being filled; rubber butyl septa was used to seal the flasks after collection and each sample were visually inspected to confirm absence of air bubbles. Metallic caps were crimped to each flask so as to avoid air exchange between the sample and ambient air. A headspace was created on each sample by replacing 10 mL of water with N₂O-free synthetic air (99.999 %, AirLiquide, Düsseldorf, Germany). Subsequently, samples were stirred using a Vortex-Genie® 2 mixer (Scientific Industries Inc., USA) and poisoned with 0.5 μ L of HgCl₂. Samples were stored at room temperature and after an equilibration time of at least 2 h were analyzed using a GC/ECD system (Hewlett Packard (HP) 5890 Series II gas chromatograph equipped with a HP 19233 ECD (Agilent Technologies, Santa Clara, CA, USA)). The separation procedure was carried out in a stainless steel column (length: 1.83 m, external diameter: 3.2 mm, internal diameter: 2.2 mm) with a molecular sieve of 5 Å (W. R. Grace and Co. Conn., Columbia, USA). At least four standard gas mixtures (the highest being 933 ppb N₂O) were used to establish calibration curves for the measurements in order to estimate the N₂O concentration from the integrated peak areas of the chromatograms. The concentration of dissolved N₂O was calculated using the expression by Walter et al. (2006).

Final absorption data from the DLT-100 is reported in terms of dry molar fraction of the corresponding gas. Thus the concentration of N₂O in seawater was calculated using

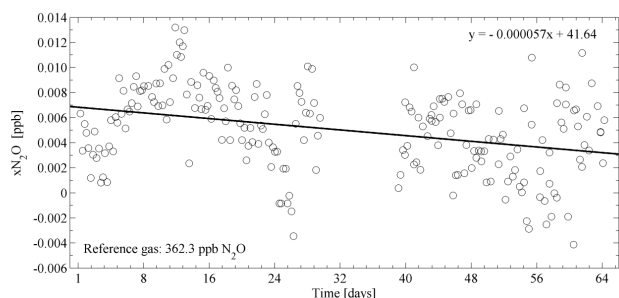


Fig. 7. N₂O standard gas measurements carried out during the MSM 18-2 and 18-3 cruises between May–July 2011. Data are presented as the deviation of every single measurement period (3 min means) from the reference value (cf. Eq. (5)). A linear regression to the data and the corresponding equation are also shown.

the expression by Weiss and Price (1980):

$$C_{N_2O} = \beta \cdot x' \cdot P, \quad (7)$$

where β is the Bunsen solubility (in mol L⁻¹ atm⁻¹) computed with the equation of Weiss and Price (1980) at equilibration temperature and in situ salinity, x' is the measured dry molar fraction of N₂O, and P the ambient pressure. Differences between in situ and equilibration temperature were taken into account by applying the correction from Walter et al. (2004):

$$C_{N_2O_{sw}} = C_{N_2O} \cdot \left(\frac{\beta_{EQ}}{\beta_{SST}} \right), \quad (8)$$

where β_{EQ} and β_{SST} are the Bunsen solubilities at equilibration and in situ temperatures, respectively. The N₂O equilibrium concentration (C_{N_2O} atm) was calculated by using measurements of ambient air carried out during the cruises and Eq. (7). N₂O saturations were computed from the ratio between $C_{N_2O_{sw}}$ and C_{N_2O} atm.

In order to compute CO₂ from in situ data, samples for dissolved inorganic carbon and total alkalinity (DIC/T_A) determinations were collected in 500 mL borosilicate glass bottles (Schott Duran®) with ground glass stoppers, and were treated according to the procedures described in Dickson et al. (2007). DIC was measured by means of the coulometric method using a Single-Operator Multi-parameter Metabolic Analyzer (SOMMA) (Johnson et al., 1993) whereas T_A was measured by potentiometric titration as described by Mintrop et al. (2000). Seawater CO₂ fugacity (fCO_2) was computed using a Microsoft Excel macro written by D. Pierrot (AOML–NOAA), which is based upon the code originally developed by Lewis and Wallace (1998). In the parameterization used, seawater pH scale (mol kg sw⁻¹) was chosen and the dissociation constants for carbonic acid (K_1 , K_2) from Mojica-Prieto and Millero (2002) were employed. The dry molar fractions of CO₂ delivered by the LI-6252 were calibrated and used to compute in situ fCO_2 according to the recommended procedures described in Dickson et al. (2007).

Concentrations of dissolved CO were computed by means of a similar expression as in Eq. (7), but with the addition of a correction for water vapor effects and the Oswald solubility coefficient α . Thus, CO molar concentrations were obtained from the product of the gas partial pressure and its solubility at equilibration temperature and in situ salinity (Bates et al., 1995):

$$C_{CO} = (x' \cdot (P_a - P_w)) \cdot \alpha, \quad (9)$$

where x' is the measured gas molar fraction, P_a is the atmospheric pressure, and P_w is the saturation water vapor pressure at equilibration temperature and salinity (Weiss and Price, 1980). The solubility was calculated with the expression by Battino (1984): $\alpha = \beta \times (T_K / 273.15)$, with β being the Bunsen solubility of CO (Wiesenburg and Guinasso, 1979) and T_K the absolute temperature in the equilibrator (in K). A correction in order to account for temperature differences between the water intake and the equilibrator was performed by using the ratio of the solubilities (α) at equilibration and in situ temperatures. All values are expressed in nmol L⁻¹ after dividing C_{CO} by the molar volume of CO at standard pressure and temperature (Stubbins et al., 2006). The saturation ratios were obtained after dividing C_{CO} by the expected concentration of dissolved CO while in equilibrium with the atmosphere (Stubbins et al., 2006). Light measurements (Photosynthetically Active Radiation, PAR) were carried out along the cruise track by using a Messen Nord radiation measurement system (SMS-1 A) installed at the vessels antenna.

Measurements of discrete and underway N₂O and CO₂ were consistent, and a good linear correlation between data from both methods was found (Fig. 8). For N₂O, differences between measured values (underway – discrete) were highly variable and oscillated between -0.57 and 1.29 nmol L⁻¹ (mean 0.43 ± 0.44 nmol L⁻¹) which corresponds to deviations of 7–20%. Analysis of the regression residuals of discrete vs. underway C_{N_2O} showed values within ± 1 nmol L⁻¹ and no systematic trends of increase or decrease, indicating that these results cannot be attributed only to the differences in accuracy between the analytical methods. In GC/ECD determinations the sample collection and handling as well as the measuring procedures carried out add further uncertainty to the measurements, and thus larger errors are expected in comparison to those produced by using OA-ICOS. In the case of the data sets evaluated as part of the comparison, rejecting differences higher than 10% under the assumption of sampling/handling problems for the GC/ECD method (typical precision 0.7 nmol L⁻¹; Bange et al. (2001)) leads to 50% reduction of the mean offset, which corresponds to an average difference of 0.22 nmol L⁻¹ between underway and discrete measurements. On the other hand, it should be also considered that the samples for N₂O were always collected while the ship was steaming, which suggests that the error among replicates of a given sampling period can be increased because of the spatial separation between them. This might

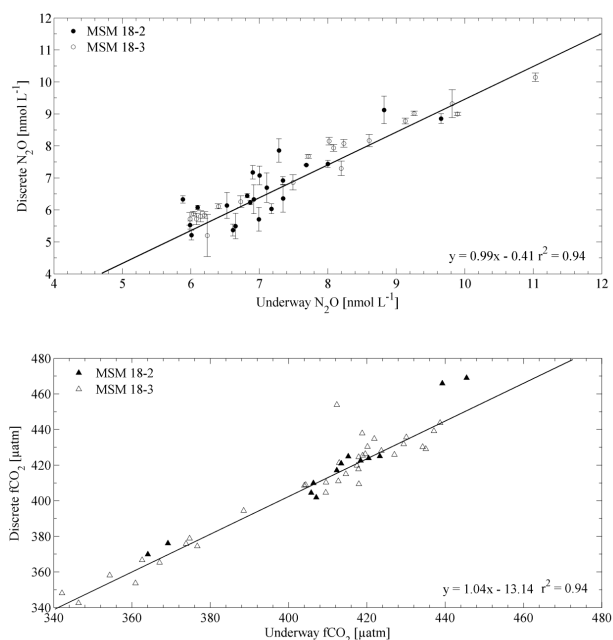


Fig. 8. Comparison of discrete and underway N₂O (top) and CO₂ (bottom) measurements during the MSM 18-2 and 18-3 cruises. A GC/ECD method was used for discrete N₂O samples whereas $f\text{CO}_2$ was calculated from discrete DIC and T_A data. Regression lines are included on each plot and, for N₂O, the standard deviation from triplicate samples is represented by vertical bars.

be particularly relevant if sharp gradients in surface seawater properties are crossed. The observation that the highest offsets in N₂O concentration coincided with steep sea surface temperature (SST) changes during both cruises supports this argument and provides indication that the divergence between the methods considered here can also be partly explained by the higher temporal resolution of the OA-ICOS instrument, since it is capable of resolving features that under a discrete sampling scheme might be either overlooked or interpreted as noise. Besides these differences, the similarity of the results obtained by the two methods indicates a good performance of the underway system.

An additional evaluation of the performance of the LI-6252 used as part of this study was carried out by running a separate underway system for CO₂ measurements from General Oceanics, Inc., USA (hereafter called GO). GO was operated in parallel to the N₂O/CO/CO₂ system using the same water source as well as the same standard mixtures of gases. A detailed description of the GO system can be found in Pierrot et al. (2009). Despite some differences in the general design and the fact that the GO system runs autonomously, the principle of measurement is the same: sample air is drawn from an equilibration chamber, detected using a NDIR gas analyzer (model LI-6262) and returned back to the chamber, forming a closed circuit. After MSM 18-2 a large leakage was detected in the internal components of the NDIR ana-

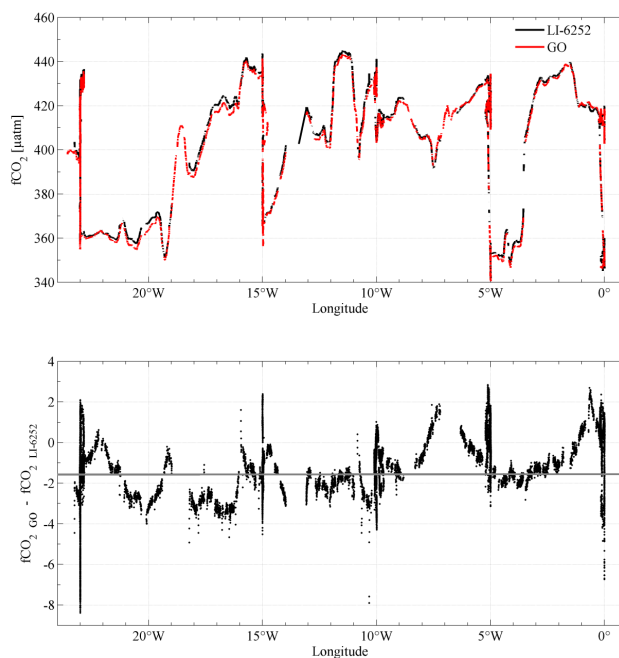


Fig. 9. Assessment of the LI-6252 performance during the MSM 18-3 cruise. A comparison of $f\text{CO}_2$ computed from GO (red line) and LI-6252 (black line) data (top) as well as the $f\text{CO}_2$ difference between both systems (bottom) is shown. The mean offset is represented by the grey line on the bottom panel.

lyzer of the GO, and therefore only data from MSM 18-3 were used for the comparison. Figure 9 shows the spatial distribution of $f\text{CO}_2$ values computed from data collected by the N₂O/CO/CO₂ system described here and the GO for a cruise track between 15° N and 5° S. The two data sets are consistent within $\pm 1.6 \mu\text{atm}$ over the whole cruise. $f\text{CO}_2$ from the sensor at the N₂O/CO/CO₂ system is somewhat higher than $f\text{CO}_2$ from GO, but nevertheless both systems agree within the recommended target of $2 \mu\text{atm}$ for high-quality oceanic CO₂ measurements (Pierrot et al., 2009). In line with these observations, the results of a regression analysis also indicated a reliable operation of the N₂O/CO/CO₂ underway system when results are compared to those delivered by GO ($y = 1.00x - 1.67$, $r^2 = 0.995$, $n = 16522$).

Measurements of atmospheric gas mixing ratios of N₂O, CO and CO₂ were in reasonably good agreement with monthly mean mixing ratios from the NOAA ESRL Carbon Cycle Cooperative Global Air Sampling Network station at Ascension Island (hereafter ASC, 7.96° S 14.4° W, http://www.esrl.noaa.gov/gmd/dv/site/site.php?code=_ASC). A summary of the results is presented in Table 2. N₂O values varied between 320.41 and 326.12 ppb, with an average monthly mean of 323.04 ± 0.96 ppb. This value is somewhat lower than the mixing ratio reported for May–July at ASC (324.09 ± 0.40 ppb; Dlugokencky et al., 2011) but the temporal and spatial trends were well

represented, with no major changes after two months of measurements and no significant latitudinal gradient. This suggests a rather uniform distribution of atmospheric N₂O over the equatorial Atlantic, which is expected due to the lack of relevant sources or sinks of this gas in the troposphere (Prather et al., 2001).

In contrast, CO gas mixing ratios were highly variable, fluctuating between 51.16 and 153.99 ppb (mean 92.92 ± 18.19 ppb) with a slight increase over time (maximum values were observed in mid-July). These results are comparable with the range of observations obtained at ASC between May and July 2011 (58.04–123.77 ppb) and also depict part of the seasonal cycle of atmospheric CO in the area, which is characterized by a sharp increase from ca. 60 ppb in May to about 120 ppb in July, when the maximum values of the annual cycle are reached (Novelli and Masarie, 2012). The CO monthly mean at ASC differs considerably from our measurements (83.20 ± 16.60 ppb), although is in the same range of uncertainty. Such dissimilarities are likely due to spatiotemporal variability which is not equally represented in the two data sets; this affects the comparison strongly because of the inherently high variability of this gas due to a marked daily cycle (Conrad et al., 1982; Table 2).

Measured mixing ratios of CO₂ were on average 2 ppm higher than those observed at ASC, and had uncertainties in the same order of magnitude (Conway et al., 2012; Table 2). This discrepancy was rather constant during the two cruises, being consistent with the observed trend at ASC between May and July when only slight changes were reported. Although no obvious system failures were detected on the NDIR analyzer or the measurement setup itself, this is not yet an automated system and because of the manual operation, higher or lower flushing times may have occurred. On the other hand, the comparatively high scatter obtained could have been due to the fact that the measuring interval was too short, generating only a few data points to produce the mean value for each measurement period. Additionally, it seems also likely that some remaining air from the equilibrator circuit could have affected the results due to the insufficient flushing of the gas lines after switching between atmospheric and oceanic measurements. Nearly 50 % of the CO₂ gas mixing ratios measured by our system were within the uncertainty of the monthly mean value recorded at ASC (387.7–391.5 ppm) which does not exclude, however, some problem with the sample handling at the control unit. Longer flushing times and/or increased pumping speed should be tested in further at-sea tests in order to improve underway CO₂ atmospheric measurements.

5 Surface seawater N₂O/CO/CO₂ measurements in the equatorial Atlantic

The two-month record of highly resolved surface water measurements was used to trace the development of the equato-

rial upwelling in the eastern tropical Atlantic Ocean. Such seasonality is mainly controlled by the strength and variability of trade winds and the meridional displacement of the Intertropical Convergence Zone (ITCZ, Philander and Pacanowski, 1986; Grodsky et al., 2008). Between March and May (ITCZ displaced northward) low wind speeds, reduced vertical transport and high surface temperatures are dominant, whereas from June to August equatorial upwelling emerges as a response to enhanced trade wind speeds, shoaling of the pycnocline and increased vertical advection of cold, nutrient-rich waters to the surface. Subsequent weakening of the winds towards September–October restores the stratified condition and sea surface temperatures increase reaching maximal values on March (Vinogradov, 1981). Figure 10 shows the computed C_{N2O} and *f*CO₂ from two equatorial sections before (EQ I, Fig. 6) and after (EQ II, Fig. 6) the onset of the equatorial upwelling (SST change from 27.16 °C on 8 June to 23.40 °C on 13 June). Evaluation of these sections for N₂O evidenced the presence of supersaturated waters with saturation levels up to 148 % (mean: 121 ± 7 %) as well as a strong correlation between C_{N2O} and SST ($r^2 = 0.99$), providing indication that enhanced surface N₂O supersaturations resulted from upwelling of N₂O-enriched waters. A similar strong correlation was found by Walter et al. (2004) in the equatorial band between 0–2° N and 23.5–26° W where it was also employed as an indicator of upwelling. Surface concentrations of N₂O increased from May to June in response to advection of cold supersaturated waters from the equatorial upwelling and higher C_{N2O} values along with elevated supersaturations were found east of 12° W on both equatorial sections (Fig. 10). The mean C_{N2O} values for the first and second equatorial sections were 7.01 ± 0.17 nmol L⁻¹ and 8.14 ± 0.87 nmol L⁻¹ respectively, indicating a 16 % enhancement for the latter. This is consistent with the observation that surface distribution of N₂O in the open ocean is predominantly driven by physical forcing (Nevison et al., 1995). Comparison of the two equatorial sections for *f*CO₂ showed increasing values from middle May to early June in association with lower temperatures as a consequence of the equatorial upwelling, and the highest values were found in the eastern side of the area covered by the cruise track, particularly in the vicinity of 12 to 10° W (Fig. 10). These results are consistent with observations reported by previous studies in the eastern tropical Atlantic Ocean (Andrié et al., 1986; Bakker et al., 1999; Lefèvre et al., 2008). A strong enhancement in surface *f*CO₂ was observed during the second equatorial section (lower right panel on Fig. 10), coinciding with the temporal progression and the spatial location of the more intense upwelling area (Grodsky et al., 2008).

Seawater CO concentrations during MSM 18-2 were highly variable, ranging from 0.12 to 1.1 nmol L⁻¹ (mean 0.37 ± 0.19 nmol L⁻¹) with saturation ratios up to 17.21 (mean 5.97 ± 3.10), indicating persistent supersaturation conditions over the time span of the cruise. These values are

Table 2. Comparison of underway atmospheric measurements carried out during the MSM 18-2 and 18-3 cruises and monthly means from the NOAA sampling location at Ascension Island (7.96° S 14.4° W). All values expressed as mean ± SD.

Time period	MSM 18-2 / 18-3			ASC		
	N ₂ O (ppb)	CO (ppb)	CO ₂ (ppm)	N ₂ O (ppb)	CO (ppb)	CO ₂ (ppm)
May 2011	322.64 ± 0.70	86.12 ± 14.45	392.21 ± 2.67	323.86 ± 0.36	75.16 ± 12.75	389.10 ± 0.81
June 2011	323.63 ± 0.99	106.07 ± 17.40	392.31 ± 2.09	324.11 ± 0.41	76.32 ± 9.63	389.33 ± 0.44
July 2011				324.29 ± 0.32	97.74 ± 15.93	390.48 ± 0.85
Overall	323.04 ± 0.96	92.92 ± 18.19	392.26 ± 2.43	324.09 ± 0.40	83.20 ± 16.60	389.64 ± 0.94

within the ranges reported for surface waters by Stubbings et al. (2006) during a south–north transect on the Atlantic Ocean (0.2–2.6 nmol L⁻¹) and by Kitidis et al. (2011) in the Mauritanian upwelling region (0.4–6.2 nmol L⁻¹). Similar seawater CO concentrations (0.40–2.4 nmol L⁻¹) were also reported for the western equatorial Pacific by Bates et al. (1993) and Mastueda et al. (2000). A strong diel cycle was observed in CO concentrations with maximum values in the afternoon (mean 0.65 ± 0.19 nmol L⁻¹) and minimum values in the early morning (mean 0.20 ± 0.08 nmol L⁻¹). An example of this daily pattern is shown in Fig. 11, where CO concentrations during a west to east equatorial section between 21° W and 10° W (EQ II, Fig. 6) are displayed. In accordance with previous studies (Conrad et al., 1982; Stubbins et al., 2006) a delay of 2–4 h between the maximal diurnal light intensity (PAR) and the maximal CO concentration was observed. Despite the fact that our observations are consistent with the expected trends in surface oceanic CO, it's worth noting that most of our values lie within the lower range of the measurements by previous studies. Potential sources of interference for the measurements could be the ship fumes during station work and concentration changes in the headspace during the time elapsed before equilibration is reached. However, as inferred from the results of atmospheric measurements, the effect of ship's emissions during the cruises was minimal, and CO production in the equilibration chamber is assumed to be negligible based on the results from Law et al. (2002) in a similar equilibration system. Furthermore, since no ancillary measurements of relevant parameters such as CDOM (chromophoric dissolved organic matter) and Chl *a* were carried out during these cruises, the differences between underway and discrete methods cannot be directly related to either of those. In addition, the absence of parallel discrete sampling for CO measurements makes it difficult to assess to which extent the results from former studies are comparable to ours because they are based on gas chromatographic methods (Conrad et al., 1982; Law et al., 2002; Stubbins et al., 2006; Day and Faloon, 2009; Kitidis et al., 2011). Therefore, future studies employing at-sea measurements of CO should also include discrete measurements

in order to directly compare the results to those from continuous measurements using OA-ICOS.

6 Summary and conclusions

A new system for underway measurements of N₂O, CO and CO₂, which combines OA-ICOS and the well-established NDIR with a Weiss-type equilibrator has been developed and tested. The gas equilibration process in the chamber employed by this system occurs at a faster rate than that of other equilibrators of similar design, with a typical response time of 2.5 min for N₂O and CO₂, and of 45 min for CO. Longer equilibration times for CO are caused by its comparatively lower solubility. The DLT-100 analyzer has been shown to be highly stable with short optimal integration times, as well as to have lower detection limits when compared to instruments using similar techniques (e.g. QCL). Furthermore, experimental results showed that the DLT-100 delivers data with precision that matches the suggested optimal precision to be achieved for highly sensitive field measurements of N₂O. A two-week calibration interval of the DLT-100 has been shown to be sufficient to obtain highly accurate N₂O and CO data. However, operation of the system in areas of elevated surface gas concentrations might require more frequent calibrations in order to ensure the same accuracy as that obtained for the lower concentration range. The analyzer's response over time can be properly described by means of quadratic functions both in the lower and upper boundaries of its operational range for N₂O and CO, such that data corrections can be performed when the desired calibration frequency cannot be achieved during field unattended deployment of the underway system.

Field performance of the N₂O/CO/CO₂ system was tested during two oceanographic campaigns on the equatorial Atlantic Ocean. Standard gas measurements of N₂O and CO were stable over a 64-day period, with an overall instrument drift lower than 1 %. Accuracy loss for CO data was encountered during MSM 18-3, probably in association with steep temperature changes from which the analyzer did not completely recover because of its continuous use at temperatures

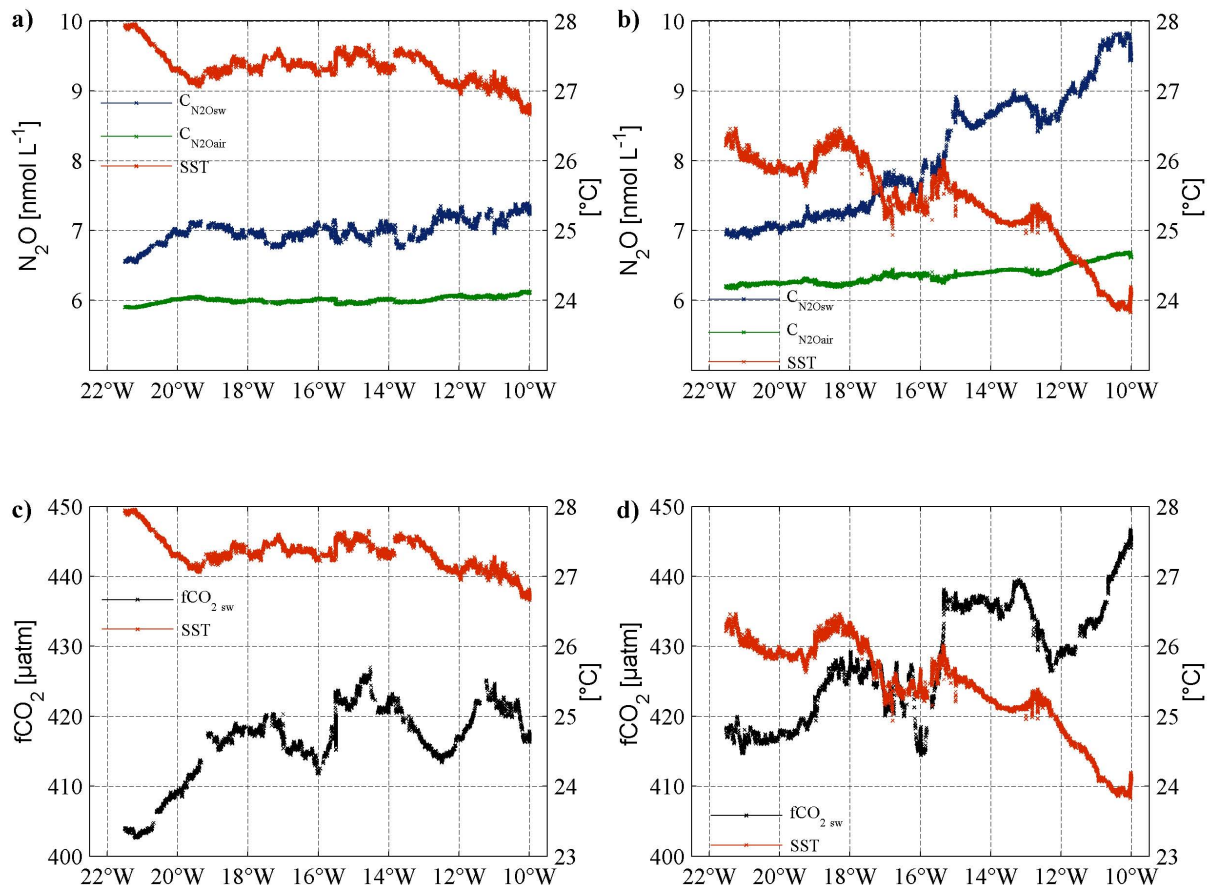


Fig. 10. Oceanic N₂O (a, b) and CO₂ (c, d) measured in two equatorial sections during the MSM 18-2 cruise (EQ I and EQ II, Fig. 6). The sections were done before (May, left) and after (June, right) the onset of the equatorial upwelling as indicated by the SST (in red). For N₂O, the equilibrium concentration (C_{N₂Oair}) is displayed in green.

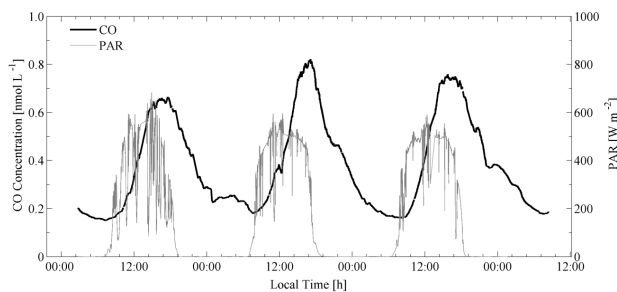


Fig. 11. CO concentration measured throughout an equatorial section (EQ II, Fig. 6) during the MSM 18-2 cruise. PAR = photosynthetically active radiation.

close to the upper boundary of its operational range. Long-term deployment of the system for at-sea measurements would therefore require appropriate ventilation of the analyzer, in particular when it is operated in warm tropical environments. Comparison of C_{N₂O} and fCO₂ data computed from measurements carried out by means of the un-

derway system described here, and discrete, well-established methods showed good agreement during both cruises, with most deviations being due to differences in the experimental setup, and in particular the sample handling. A temporal mismatch during crossing through sharp gradients also influenced the comparison by reducing the precision of the discrete methods. Furthermore, the functioning of the NDIR analyzer while coupled into the N₂O/CO/CO₂ system was tested by direct comparison with the autonomous GO system. Results showed a remarkable agreement between setups, suggesting a reliable operation of our underway analytical system.

Results from atmospheric measurements agree reasonably well with monthly means of the NOAA atmospheric sampling location at Ascension Island, although further technical modifications are required in order to improve the obtained accuracy. A two-month record of N₂O and CO₂ was used to trace the development of the equatorial upwelling in the Atlantic Ocean, providing the first high-resolution view of the temporal and spatial surface distribution patterns of these two climate-relevant gases in the area. Moreover, concentrations

of dissolved N₂O, CO and CO₂ during the MSM 18-2 cruise were in good agreement with those reported in previous studies in different oceanic areas. The overall accuracy of CO measurements, however, is yet to be tested by direct comparison with traditional discrete methods. These results put forward the potential of the underway method employed as a tool to unravel fine-scale biological and physical processes on the surface ocean which might be otherwise ignored due to lack of resolution.

In conclusion, this new setup used to perform simultaneous underway N₂O, CO and CO₂ measurements has been shown to have good short and long-term stability, accuracy, and improved precision in comparison with systems based upon similar infrared techniques and traditional discrete methods (for N₂O and CO₂). Further work is required in order to validate the accuracy of oceanic CO measurements, however. The relatively simple setup performed well during its first major field deployment in the equatorial Atlantic Ocean, thus suggesting its potential to be used continuously not only onboard research vessels but also on voluntary observing ships (VOS).

Acknowledgements. We are very grateful to A. Jordan for the calibration of our standard gases at the Max Planck Institute for Biogeochemistry, Jena. Moreover, we thank Los Gatos Research Inc. for their continuous support during the setup of the system. We thank the captain and crew of R/V *Maria S. Merian* for their support during the cruise MSM 18, legs 2 and 3. We also thank P. Brandt for his support during the MSM 18-2 cruise, and B. Fiedler, S. Fessler and T. Baustian for providing technical support during the cruises as well as the measurement and analysis of DIC/T_A and N₂O samples. The work presented here was made possible by generous funding from the Future Ocean Excellence Cluster at Kiel University (project CP0910), the BMBF joint project SOPRAN II (FKZ 03F0611A) and the EU FP7 project InGOS (grant agreement no 284274).

The service charges for this open access publication have been covered by a Research Centre of the Helmholtz Association.

Edited by: M. Hoppema

References

- Allan, D. W.: Statistics of atomic frequency standards, *Proc. IEEE*, 54, 221–230, 1966.
- Andrié, C., Oudot, C., Genthon, C. and Merlivat, L.: CO₂ fluxes in the tropical Atlantic during FOCAL cruises, *J. Geophys. Res.*, 21, 11741–11755, 1986.
- Baer, D. S., Paul, J. B., Gupta, M., and O'keefe, A.: Sensitive absorption measurements in the near-infrared region using off-axis integrated-cavity output spectroscopy, *Appl. Phys. B.*, 75, 261–265, 2002.
- Bakker, D. C. E., de Baar, H. J. W., and de Jong, E.: Dissolved carbon dioxide in tropical east Atlantic surface waters, *Phys. Chem. Earth*, 24, 399–404, 1999.
- Bange, H. W., Rapsomanikis, S., and Andreae, M. O.: Nitrous oxide in coastal waters, *Global Biogeochem. Cy.*, 10, 197–207, 1996a.
- Bange, H. W., Rapsomanikis, S., and Andreae, M. O.: The Aegean Sea as a source of atmospheric nitrous oxide and methane, *Mar. Chem.*, 53, 41–49, 1996b.
- Bange, H. W., Rapsomanikis, S., and Andreae, M. O.: Nitrous oxide cycling in the Arabian Sea, *J. Geophys. Res.*, 106, 1053–1065, 2001.
- Bates, T. S., Kelly, K. C., and Johnson, J. E.: Concentrations and fluxes of dissolved biogenic gases (DMS, CH₄, CO, CO₂) in the equatorial Pacific during the SAGA 3 experiment, *J. Geophys. Res.*, 98, 16969–16977, 1993.
- Bates, T. S., Kelly, K. C., Johnson, J. E., and Gammon, R. H.: Regional and seasonal variations in the flux of oceanic carbon monoxide to the atmosphere, *J. Geophys. Res.*, 100, 23093–23101, 1995.
- Battino, R.: The Ostwald coefficient of gas solubility, *Fluid Phase Equilibr.*, 15, 231–240, 1984.
- Becker, M., Andersen, N., Fiedler, B., Fietzek, P., Körtzinger, A., Steinhoff, T., and Friedrichs, G.: Using cavity ringdown spectroscopy for continuous monitoring of δ¹³C(CO₂) and *f*CO₂ in the surface ocean, *Limnol. Oceanogr. Methods*, 10, 752–766, 2012.
- Burch, D. E., Singleton, E. B., and Williams, D.: Absorption line broadening in the infrared, *Appl. Optics*, 1, 359–363, 1962.
- Butler, J. H., Elkins, J. W., Brunson, C. H., Egan, K. B., Thompson, T. M., Conway, T. J., and Hall, B. D.: Trace gases in and over the West Pacific and East Indian Oceans during the El Niño-Southern Oscillation event of 1987, *Data Rep. ERL ARL-16, Air Resour. Lab., Natl. Oceanic and Atmos. Admin., Silver Spring, Maryland*, 104 pp., 1988.
- Conrad, R., Seiler, W., Bunse, G., and Giehl, H.: Carbon monoxide in seawater (Atlantic Ocean), *J. Geophys. Res.*, 87, 8839–8852, 1982.
- Conway, T. J., Lang, P. M., and Masarie, K. A.: Atmospheric carbon dioxide dry air mole fractions from the NOAA ESRL Carbon Cycle Cooperative Global Air Sampling Network, 1968–2011, <ftp://ftp.cmdl.noaa.gov/ccg/co2/flask/event/> last access: May 2013, version: 15.08.2012, 2012.
- Day, D. A. and Faloona, I.: Carbon monoxide and chromophoric dissolved organic matter cycles in the shelf waters of the northern California upwelling system, *J. Geophys. Res.*, 114, C01006, doi:10.1029/2007JC004590, 2009.
- Denman, K. L., Brasseur, G., Chidthaisong, A., Ciais, P., Cox, P. M., Dickinson, R. E., Hauglustaine, D., Heinze, C., Holland, E., Jacob, D., Lohmann, U., Ramachandran, S., da Silva Dias, P. L., Wofsky, S. C., and Zhang, X.: Couplings between changes in the climate system and biogeochemistry, in: *Climate change 2007, the physical science basis, contribution of working group I to the Fourth Assessment Report of the Intergovernmental Panel on Climate Change*, edited by: Solomon, S., Qin, D., Manning, M., Chen, Z., Marquis, M., Averyt, K. B., Tignor, M., and Miller, H. L., Cambridge University Press, Cambridge, United Kingdom and New York, NY, USA, 499–587, 2007.

- Dickson, A. G., Sabine, C. L., and Christian, J. R.: Guide to best practices for ocean CO₂ measurements, PICES Special Publication, 3, 191 pp., 2007.
- Dlugokencky, E. J., Lang, P. M., and Masarie, K. A.: Atmospheric N₂O dry air mole fractions from the NOAA GMD Carbon Cycle Cooperative Global Air Sampling Network, 1997–2010, version: 9.11.2011, 2011.
- Dyroff, C.: Optimum signal-to-noise ratio in off-axis integrated cavity output spectroscopy, *Opt. Lett.*, 36, 1110–1112, 2011.
- Forster, P., Ramaswamy, V., Artaxo, P., Bernsten, T., Betts, R., Fahey, D. W., Haywood, J., Lean, J., Lowe, D. C., Myhre, G., Nganga, J., Prinn, R., Raga, G., Schulz, M., and Van Dorland, R.: Changes in atmospheric constituents and in radiative forcing, in: *Climate change 2007, the physical science basis, contribution of working group I to the Fourth Assessment Report of the Intergovernmental Panel on Climate Change*, edited by: Solomon, S., Qin, D., Manning, M., Chen, Z., Marquis, M., Averyt, K. B., Tignor, M., and Miller, H. L., Cambridge University Press, Cambridge, United Kingdom and New York, NY, USA, 129–234, 2007.
- Friedrichs, G.: Sensitive absorption methods for quantitative gas phase kinetic measurements, Pt. 2: Cavity ringdown spectroscopy, *Z. Phys. Chem.*, 222, 31–61, 2008.
- Grefe, I. and Kaiser, J.: Equilibrator-based measurements of dissolved nitrous oxide in the surface ocean using an integrated cavity output laser absorption spectrometer, *Ocean Sci. Discuss.*, 10, 1031–1065, doi:10.5194/osd-10-1031-2013, 2013.
- Grodsky, S. A., Carton, J. A., and McClain, C. R.: Variability of upwelling and chlorophyll in the equatorial Atlantic, *Geophys. Res. Lett.*, 35, L03610, doi:10.1029/2007GL032466, 2008.
- Gülzow, W., Rehder, G., Schneider, B., Schneider, J., Deimling, V., and Sackowiak, B.: A new method for continuous measurement of methane and carbon dioxide in surface waters using off-axis integrated cavity output spectroscopy (ICOS), An example from the Baltic Sea, *Limnol. Oceanogr.*, 9, 176–184, 2011.
- Gülzow, W., Rehder, G., Schneider v. Deimling, J., Seifert, T., and Tóth, Z.: One year of continuous measurements constraining methane emissions from the Baltic Sea to the atmosphere using a ship of opportunity, *Biogeosciences*, 10, 81–99, doi:10.5194/bg-10-81-2013, 2013.
- Hendriks, D. M. D., Dolman, A. J., van der Molen, M. K., and van Huissteden, J.: A compact and stable eddy covariance set-up for methane measurements using off-axis integrated cavity output spectroscopy, *Atmos. Chem. Phys.*, 8, 431–443, doi:10.5194/acp-8-431-2008, 2008.
- Herriott, D., Kogelnik, H., and Kompfner, R.: Off-axis paths in spherical mirror interferometers, *Appl. Optics*, 3, 523–526, 1964.
- Hupp, J.: The importance of water vapor measurements and corrections, Application note # 129 v. March 2010, LI-COR Biosciences Inc., 8 pp., 2011.
- Johnson, J. E.: Evaluation of a seawater equilibrator for shipboard analysis of dissolved oceanic trace gases, *Anal. Chim. Acta*, 395, 119–132, 1999.
- Johnson, K., Willis, K., Butler, D., Johnson, W., and Wong, C.: Coulometric total carbon dioxide analysis for marine studies: maximizing the performance of an automated gas extraction system and coulometric detector, *Mar. Chem.*, 44, 167–187, 1993.
- Kasyutich, V. L., Bale, C. S. E., Canosa-Mas, C. E., Perang, C., Vaughan, S., and Wayne, R. P.: Cavity-enhanced absorption: detection of nitrogen dioxide and iodine monoxide using a violet laser diode, *Appl. Phys. B*, 76, 691–697, 2003.
- Kitidis, V., Tilstone, G. H., Smyth, T. J., Torres, R., and Law, C. S.: Carbon monoxide emission from a Mauritanian upwelling filament, *Mar. Chem.*, 127, 123–133, 2011.
- Körtzinger, A., Thomas, H., Schneider, B., Gronau, N., Mintrop, L., and Duinker, J. C.: At sea intercomparison of two newly designed underway pCO₂ systems – encouraging results, *Mar. Chem.*, 52, 133–145, 1996.
- Körtzinger, A., Mintrop, L., Wallace, D. W. R., Johnson, K. M., Neil, C., Tilbrook, B., Towler, P., Inoue, H. Y., Ishii, M., Shaffer, G., Torres Saavedra, R. F., Ohtaki, E., Yamashita, E., Poisson, A., Brunet, C., Schauer, B., Goyet, C., and Eiseid, G.: The international at-sea intercomparison of fCO₂ systems during the R/V *Meteor Cruise 36/1* in the North Atlantic Ocean, *Mar. Chem.*, 72, 171–192, 2000.
- Kroon, P. S., Hensen, A., Jonker, H. J. J., Zahniser, M. S., van't Veen, W. H., and Vermeulen, A. T.: Suitability of quantum cascade laser spectroscopy for CH₄ and N₂O eddy covariance flux measurements, *Biogeosciences*, 4, 715–728, doi:10.5194/bg-4-715-2007, 2007.
- Law, C. S., Sjöberg, T. N., and Ling, R. D.: Atmospheric emission and cycling of carbon monoxide in the Scheldt estuary, *Biogeochemistry*, 59, 69–94, 2002.
- Lefèvre, N., Guillot, A., Beaumont, L., and Danguy, T.: Variability of fCO₂ in the eastern tropical Atlantic from a moored buoy, *J. Geophys. Res.*, 113, C01015, doi:10.1029/2007JC004146, 2008.
- Lewis, E. and Wallace, D. W. R.: Program developed for CO₂ system calculations. ORNL/CDIAC-105, Carbon Dioxide Information and Analysis Center, Oak Ridge National Laboratory, US Department of energy, Oak Ridge, 1998.
- LI-COR: LI-6252 CO₂ analyzer operating and service manual, LI-COR Biosciences Inc., Publication No. 9003-60, Lincoln, Nebraska, USA, 121 pp., 1996.
- Maddaloni, P., Gagliardi, G., Malara, P., and De Natale, P.: Off-axis integrated-cavity-output spectroscopy for trace-gas concentration measurements, modeling and performance, *J. Opt. Soc. Am. B*, 23, 1938–1945, 2006.
- Matsueda, H., Inque, H. Y., Asanuma, I., Aoyama, M., and Ishii, M.: Carbon monoxide and methane in surface seawater of the tropical Pacific Ocean, in: *Dynamics and characterization of marine organic matter*, edited by: Handa, N., Tanoue, E., and Hama, T., Terrapub/Kluwer, Japan, 485–508, 2000.
- Mazurenka, M., Orr-Ewing, A. J., Pervall, R., and Ritchie, G. A. D.: Cavity ringdown and cavity enhanced spectroscopy using diode lasers, *Annu. Rep. Prog. Chem. C*, 101, 100–142, 2005.
- McDermitt, D. K., Welles, J. M., and Eckles, R. D.: Effects of temperature, pressure and water vapor on gas phase infrared absorption by CO₂, LI-COR Biosciences, Inc., 5 pp., 1993.
- Mintrop, L., Pérez, F. F., González-Dávila, M., Santana-Casiano, J. M., and Körtzinger, A.: Alkalinity determination by potentiometry, intercalibration using three different methods, *Cienc. Mar.*, 26, 23–37, 2000.
- Mojica-Prieto, F. J. and Millero, F. J.: The values of pK₁ + pK₂ for the dissociation of carbonic acid in seawater, *Geochim. Cosmochim. Acta*, 66, 2529–2540, 2002.
- Nelson, D. D., McManus, B., Urbanski, S., Herndon, S., and Zahniser, M. S.: High precision measurements of nitrous oxide and methane using thermoelectrically cooled mid-infrared quantum

- cascade lasers and detectors, *Spectrochim. Acta A.*, 60, 3325–3335, 2004.
- Nevison, C. D., Weiss, R. F., and Erikson III, D. J.: Global oceanic emissions of nitrous oxide, *J. Geophys. Res.*, 100, 15809–15820, 1995.
- Novelli, P. C. and Masarie, K. A.: Atmospheric carbon monoxide dry air mole fractions from the NOAA ESRL Carbon Cycle Cooperative Global Air Sampling Network, 1988–2011, <ftp://ftp.cmdl.noaa.gov/ccg/co/flask/event/> last acces: May 2013, version: 18.09.2011, 2012.
- O’Keefe, A. and Deacon, D. A. G.: Cavity ring-down optical spectrometer for absorption measurements using pulsed laser sources, *Rev. Sci. Instrum.*, 59, 2544–2551, 1988.
- Paul, J. B., Lapson, L., and Anderson, J. G.: Ultrasensitive absorption spectroscopy with a high-finesse optical cavity and off-axis alignment, *Appl. Optics*, 40, 4904–4910, 2001.
- Philander S. G. H. and Pacanowski, R. C.: A model of the seasonal cycle in the Tropical Atlantic Ocean, *J. Geophys. Res.*, 91, 14192–14206, 1986.
- Pierrot, D., Neill C., Sullivan, K., Castle, R., Wanninkhof, R., Lüger, H., Johannessen, T., Olsen, A., Feely, R. A., and Cosca, C. E.: Recommendations for autonomous underway pCO₂ measuring systems and data-reduction routines, *Deep-Sea Res. Pt.II*, 56, 512–522, 2009.
- Prather, M., Ehhalt, D., Dentener, F., Derwent, R., Dlugokencky, E., Holland, E., Isaksen, I., Katima, J., Kirchhoff, V., Matson, P., Midgley, P., and Wang, M.: Atmospheric chemistry and greenhouse gases, in: *Climate change 2001, the physical science basis, contribution of working group I to the Third Assessment Report of the Intergovernmental Panel on Climate Change*, edited by: Houghton, J. T., Ding, Y., Griggs, D. J., Noguer, M., van der Linden, P. J., Dai, X., Maskell, K., and Johnson, C. A., Cambridge University Press, Cambridge, United Kingdom and New York, NY, USA, 239–287, 2001.
- Stubbins, A., Uher, G., Kitidis, V., Law, C. S., Upstill-Goddard, R. C., and Woodward, E. M. S.: The open-ocean source of atmospheric carbon monoxide, *Deep-Sea. Res. Pt.II*, 53, 1685–1694, 2006.
- Vinogradov, M.: Ecosystems of equatorial upwellings, in: *Analysis of marine ecosystems*, edited by: Longhurst, A. R., Academic Press, London, 69–93, 1981.
- Walter, S., Bange, H. W., and Wallace, D. W. R.: Nitrous oxide in the surface layer of the tropical North Atlantic Ocean along a west to east transect, *Geophys. Res. Lett.*, 31, L23S07, doi:10.1029/2004GL019937 2004.
- Walter, S., Bange, H. W., Breitenbach, U., and Wallace, D. W. R.: Nitrous oxide in the North Atlantic Ocean, *Biogeosciences*, 3, 607–619, doi:10.5194/bg-3-607-2006, 2006.
- Weiss, R. F.: Carbon dioxide in water and seawater, the solubility of a non-ideal gas, *Mar. Chem.*, 2, 203–215, 1974.
- Weiss, R. F.: Determinations of carbon dioxide and methane by dual catalyst flame ionization chromatography and nitrous oxide by electron capture chromatography, *J. Chromatogr. Sci.*, 19, 611–616, 1981.
- Weiss, R. F. and Price, B. A.: Nitrous oxide solubility in water and seawater, *Mar. Chem.*, 8, 347–359, 1980.
- Weiss, R. F., Van Woy, F. A., and Salameh, P. K.: Surface water and atmospheric carbon dioxide and nitrous oxide observations by shipboard automated gas chromatography, results from expeditions between 1977 and 1990, *Scripps Instit. Oceanogr. Ref. 92-11*, Scripps Institution of Oceanography, San Diego, USA, 1992.
- Werle, P., Mücke, R., and Slemr, F.: The limits of signal averaging in atmospheric trace-gas monitoring by tunable diode-laser absorption spectroscopy (TDLAS), *Appl. Phys. B.*, 57, 131–139, 1993.
- Wiesenburg, D. A. and Guinasso, Jr., N. L.: Equilibrium solubilities of methane, carbon monoxide, and hydrogen in water and sea water, *J. Chem. Eng. Data*, 24, 356–360, 1979.
- Wilhelm, E., Battino, R., and Wilcock, R. J.: Low-pressure solubility of gases in liquid water, *Chem. Rev.*, 77, 219–262, doi:10.1021/cr60306a003, 1977.
- Zellweger, C., Steinbacher, M., and Buchmann, B.: Evaluation of new laser spectrometer techniques for in-situ carbon monoxide measurements, *Atmos. Meas. Tech.*, 5, 2555–2567, doi:10.5194/amt-5-2555-2012, 2012.